AUT Journal of Electrical Engineering

AUT J. Elec. Eng., 56(1) (Special Issue) (2024) 125-140
DOI: 10.22060/eej.2024.22513.5544

Optimization and Torque Improvement of a Salient-Pole Permanent Magnet Synchronous Machine by Three-step Skewed Pole Shoe Method

H. Parivar*, A. Darabi

Department of Electrical Engineering, Shahrood University of Technology, Shahrood, Iran

ABSTRACT: In this paper, a novel method to design and optimization of a 1.5 kW, 4-pole, 36-slot salient-pole permanent magnet synchronous machine (SPPMSM) based on a three-step skewed pole shoe method to reduce the output torque ripple and the cogging torque is investigated. In the first step, an initial model of the SPPMSM is designed, simulated, and verified through the Finite-Element method (FEM). The simulation results ensure the electromagnetic performance of the initial model of the machine under any operating conditions. Next, a novel method to re-design and optimize the SPPMSM based on a three-step skewed pole shoe shape is presented.. The significant results obtained from the optimized model of the SPPMSM are as: The output average torque and the air gap flux density are increased approximately by 12.65% and 3.33%, respectively compared to the initial design of the SPPMSM. The torque ripple is an important parameter in the design of the machine, and so, is decreased by about 16.03% which is equal to 10.41% in comparison with the initial model which is equal to 12.41%. The cogging torque in the initial model of the SPPMSM is equal to 0.036 N.m and with a 19.44% reduction, in the optimized model, it is 0.029 N.m. And finally, the back-EMF voltage of the SPPMSM is improved by 1.27% compared to the initial design model.

Review History:

Received: Jun. 27, 2023
Revised: Dec. 29, 2023
Accepted: Jan. 06, 2024
Available Online: Feb. 01, 2024

Keywords:

Salient-pole Permanent Magnet Synchronous Machine
Skew-pole Method
Torque Ripples
Cogging Torque
Finite-element Method

1- Introduction

Relying on the advantages of the Salient-Pole Permanent Magnet Synchronous Machines (SPPMSM) such as high efficiency and power density, high power factor, and low vibration and noise, make these machines applicable in industrial, commercial, and even home applications. SPPMSMs are a type of synchronous machine which are used after the discovery of the permanent magnet (PM) materials. Over recent years, taking account of the increase in the application of the aforementioned machines, optimal design of the SPPMSM is a more attractive and challenging issue for electrical machine designers. In this manner, in various papers, the electromagnetic design of such machines is presented and various parameters such as cogging torque and torque ripple are optimized. Fortunately, the optimization and design strategies of the SPPMSMs is improving in recent years. For example, in [1] a hierarchical-like fuzzy controller is used in a salient pole permanent magnet synchronous motor (SPPMSM) by aiming to reduce the torque ripple. It should be noted that one of the advantages of the fuzzy controllers, which are introduced in [1] is that it is developed without the requirement of the machine model. The proposed approach presented in [1], compared to the conventional ones of torque ripple reduction, can reduce torque ripple by approximately 30%. It is obvious that the magnetic analysis and the air-gap field distribution in electrical machines are the main keys to recognizing the operation of the machine and then designing and optimization [2]. It also determines the necessary operating parameters for instance electromagnetic torque which is one of the important parameters for optimizing SPPMSMs. Therefore, in the SPPMSMs it is necessary to have a model to accurately describe the performance of the abovementioned machines. In [3], an extended analytical model is presented to analyze the airgap flux density in the SPPMSMs. So, in [3] a 4-poles SPPMSM is presented and investigated by means of an extended analytical model. Moreover, Air-gap MMF harmonic distribution, stator slotting, and also saliency effect of the SPPMSMs are analyzed and studied. Both no-load and under-load operation condition is done to exhibit the rotor saliency effect and stator slotting ones in 4-poles SPPMSM. Further studies also show the effect of rotor pole shape in two parameters like electromagnetic torque and the air-gap flux density of the 4-poles SPPMSM and resulted in [3] that the rotor pole shape of the 4-poles SPPMSM is sensitively affected on the rotor saliency additional harmonics and air gap flux density. The result obtained from [3] is so important to optimally design SPPMSMs by reducing the important parameters affected in SPPMSMs operation like torque ripple, cogging torque, air gap flux density, and so on. Almost in all applications, the torque ripple and cogging torque play a basic role in the performance of the PM machines [4], [5], and also, the rotor pole shoe shape of such machines has a direct effect

*Corresponding author's email: hosseinparivar72@yahoo.com

on these parameters. The expected purpose of these machines is the least amount in both torque ripple and cogging torque. In various papers, proposed electromagnetic design methods are presented to reduce torque ripple and cogging torque in PM machines like [6]–[13]especially for the ones with unevenly distributed split teeth (UDST. The proposed and more practically industry-accepted method for cogging torque and torque ripple reduction in PM machines is rotor step-skewing [4], [14]–[17]. As the rotor step-skewing increases, the torque ripple also reduces but the assembly and manufacturing costs increase. As said, another way to minimize the torque ripple in the PM machines is step-skewing by selecting a proper shape for PMs. Minimized torque ripple archives by the optimum skew angle gained by various methods. Notwithstanding, this is a sensitive way because a non-optimum skew angle produces an increased torque ripple so the magnet shape should be selected carefully. Another noted method to reduce the cogging torque and torque ripple is the rotor pole shoe shape. The step pole-shoe shape method reduces torque ripple through the reduction of average torque. But this method needs a tread-off between the magnet skewing angle and the number of steps. Like the previous approach, As to be noted, increasing the number of steps led to an increase in the output torque with the reduction in torque ripple but it is not easy to assemble. Table 1 summarized the recently presented approach to optimization of the PM machines by reducing the torque ripple and cogging torque, improving the torque characteristics, etc, in the kinds of literature.

The synchronous reluctance machine (SynRM), the Brushless DC Machine (BLDC), and the permanent magnet synchronous machine (PMSM) are good rivals for commercial, industrial, and home applications. An advantage of a SynRM is its low-cost structure, although its torque density is not as high as a PMSM. The disadvantage is that the most effective topology in SynRMs is the four-pole structure because this arrangement ensures a high inductance difference in SynRMs. This characteristic makes them suitable for geared high-speed operation and, hence, unsuitable for direct-drive applications requiring light machine structure. In this paper, the key target of the SPPMSM design, besides the direct drive, is to achieve a light structure with an enhanced output torque with inherent saliency with a proper pole design.

This paper aims to design, simulate, analyze, and optimization of an SPPMSM. In this way, a SPPMSM is initially designed, simulated through the JMAG Designer platform, and verified by employing the FEM. Then in the second step, by presenting a three-step skewed pole shoe method named:

- Right-skewed pole-shoe shape
- Left-skewed pole-shoe shape
- Fully-skewed pole-shoe shape,

is presented and analyzed to select the more proper ones that verify and ensure the electromagnetic performance of the aforementioned machine through FEM.

The rest of this paper is categorized into 8 Sections. Section II presents an SPPMSM design algorithm. The SPPMSM initial design and the proposed method are the subjects of Section III and Section IV, respectively. After Section III an initial design of SPPMSM is done, and concerning the proposed method presented in Section IV, both topics are compared in Section V, to determine a proper design scheme for the SPPMSM. Section VI covers the FEM results of the final and optimized SPPMSM, and lastly, Section VII is the conclusion

Table 1. Proposed Methods Presented in the Literature to Optimization of the PM Machines

Article.	Proposed method	Achievements	Year of Pub.
[1]	Hierarchical-like Fuzzy Controller Method	Reduction of the Torque Ripple	2021
[4]	Skew Angle Optimization Method	Reduction of Cogging Torque and Torque Ripple.	2019
[16]	Variable Magnet Step-Skew Method	Reduction of the Cogging Torque and Torque Pulsations	2020
[6]	Unevenly-distributed Split Teeth Method	Reduction of Cogging Torque and Torque Ripple.	2022
[7]	Asymmetric Pole Shaping Method	Reduction of the Torque Ripple	2022
[8]	Magnetic Field Energy Equivalence Method	Reduction of the Cogging Torque	2021
[9]	Improved Stator/Rotor-Pole Number Combinations Method	Reduction of the Torque Ripple	2021

[10]	Analytical Sub-domain Method	Reduction of the Torque Ripple	2021
[11]	Right-angled Trapezoidal Magnet Shape Method	Reduction of Cogging Torque and Torque Ripple.	2021
[18]	Stepping Air-gap and Auxiliary Teeth Method	Reduction of Cogging Torque and Torque Ripple.	2020
[13]	Advanced Step-Skewed Rotor Method	Reduction of the Torque Ripple	2022
[14]	Skew Angle Optimization	Reduction of Cogging Torque and Torque Ripple.	2016
[14], [15]	Herringbone Rotor Step Skewing	Reduction of the Torque Ripple	2016, 2013
[17]	Skew Angle Optimization Method	Improvement EMF and Output Torque and Reduction the Cogging Torque	2018
[19]	Proposed Slot Structure Method	Reduction of Cogging Torque and Torque Ripple.	2021
[20]	Optimal Shape Method	Low Pulsating Torque	2006
[21]	Harmonic Injected Current Method	Reduction of the Torque Ripple	2008
[22]	Mont-Carlo Optimization Method	Reduction of the Torque Ripple	2010
[23]	Level Set Method	Reduction of the Cogging Torque	2010
[24]	Notches Method	Reduction of the Cogging Torque	2007
[25]	Pole arc to pole pitch ratio Method	Reduction of the Torque Ripple and Improve the Back-EMF	2007
[26]	Global Stochastic Minimization Method	Reduction of the Cogging Torque	1999
[27]	Conformal Transformation Method	Reduction of the Torque Ripple	2009
[28]	Magnet-shape Optimization Method	Reduced Torque Ripple without Significant Reduction in Average Torque	2009
[29]	Maxwell stress Tensor Method	Reduction of the Cogging Torque	2008
[30]	Graph-based Method	Reduction of the Cogging Torque and Optimization the Pole Embrace Value	2019
[31]	Energy Method	Reduction of the Cogging Torque	2019
[32]	Fourier Expansion and Energy Method	Reduction of the Cogging Torque	2003
[33]	Rotor Pole Skewing Method	Low Pulsating Torque	2009
[34]	Response Surface, Kriging and Steepest Descent Method	Reduction of the Cogging Torque	2015
[35]	Steepest Descent and Response Surface Method	Reduction of the Cogging Torque	2016

Table 2. Proposed tangential Stress for SPPMSMP

SPMSM Type	σ_{tan} *(kPa)*
Ferrite-based Small SPPMSM	3.4-6.9
Rare-earth Magnet NdFeB* and SMCo**-based SPPMSM	6.9-20.6
NdFeB-based SPPMSM	~ 10.3
*** Neodymium iron boron, ** Samarium Cobalt**	

Table 3. Proposed Current Density for SPPMSM

SPMSM Type	**Current Density (*A/mm²*)**
Small TE* SPPMSM Air cooling	3-5
TE* SPPMSM with Fan-assembled Air cooling	5-10
SPPMSM with Coolant Cooling (direct water)	7-10

Table 4. Proposed values for rr/l′ Based on the SPPMSM Number of Pole Pairs

SPMSM Type	**Current Density (*A/mm²*)**
Small TE* SPPMSM Air cooling	3-5
TE* SPPMSM with Fan-assembled Air cooling	5-10
SPPMSM with Coolant Cooling (direct water)	7-10

2- SPPMSM Design Algorithm

In this part, the design parameters of the SPPMSM are presented. The initial parameters of the SPPMSM should be first determined as:

- Average (T_{avg}) and maximum torque (T_{max})
- Maximum rotational speed (n_{max}) and rated speed (n_n)
- Voltage (V_L) and current (I_L)
- Machine limitations such as machine length (l_m) and diameter (D_m)

The torque equation for an SPPMSM is presented as (1) which depends on the effective axial length of the rotor (l'_r), the rotor radius (r_r), the active area of the rotor cylinder of the SPPMSM (S_r), and the tangential stress (σ_{tan}) which defined as Table 2 in based on SPPMSM types.

$$T = \sigma_{\tan} r_r 2\pi r_r l'_r = \sigma_{\tan} S_r r_r \quad (1)$$

Table 3 also presented the proposed current density (A) for SPPMSM. Furthermore, the proposed value for the r_r/l' parameter (SPPMSM radius of the rotor per the effective axial length of the rotor) owing to the SPPMSM number of pole poles (p) is classified in Table 4. As it is noted, a large number of pole poles (p) reduce the rotational speed and the p=1 or 2, usually used for the high-speed SPPMSMs.

The Electromagnetic design of the SPPMSM complements the initial design of the PMSM and defines the dimensions of the SPPMSMs. So nextly, the further parameters of the SPPMSM are defined. After determining the initial designing value of the SPPMSM, the airgap flux is as follows:

$$\hat{\Phi} = \alpha_i \hat{B}_\delta \frac{2\pi r_\delta}{2p} l' \quad (2)$$

Where $2\pi r_\delta/2p=\tau_p$ is pole pitch, α_i is the average value per flux density in a pole and a sinusoidal flux density is equal to π/2. The maximum air gap flux density (B_δ) is an important factor in the optimum design of SPPMSMs and is selected at the value of 0.8~1.05^T, in the designing of the SPPMSMs, it is usually implied to equal to 0.9^T. The combination of the slot number (N_s) and the number of pole pairs (p) can be appointed as fractional-slot winding that the number of slots per pole per phase (q) is fractional and superior to 1. The further fractional-slot winding feature is the reduction in winding length and its economic restriction that make this type of winding appropriate for use in SPPMSM. This winding also reduces the cogging torque of the SPPMSMs. Defined the type of the SPPMSM winding to form the harmonic content of the SPPMSM current. For example by increasing the q, the value of the main component of the current decreases

and leads to a decrease in harmonics. For example, at *q=2*, the 5th and 7th harmonics decreased by 74.1% compared to *q=1* in an SPPMSM equal operation condition. So, a proper and optimal value should be selected in the initial design of SPPMSM to accomplish interaction between SPPMSM parameters. After determining the winding of the SPPMSM, its magnetic circuit should also be specified. The magnetic circuit refers to the dimensions, form, and type of iron used in SPPMSM. This parameter is affected by the current density in SPPMSM because determines the stator and rotor yoke, stator teeth, slots dimensions, etc. In this way, the flux density of SPPMSM depends on the PM, and generally in SPPMSMs is set at about 1.5T or less, based on the BH curve. The peak flux density in a stator tooth (B_d) can be modeled as (3) assuming that saturation does not occur.

$$B_d = \frac{\tau_u l'}{k_{Fe} l' b_d} B_\delta \tag{3}$$

Where τ_u, k_{Fe}, b_d and l' are the slot pitch, the iron core filling factor, teeth width, and effective stack length respectively. Additionally, (4) and (5) yield the SPPMSM the stator thickness ($h_{y,s}$), and the rotor thickness ($h_{y,r}$), respectively.

$$h_{y,s} = \frac{\hat{\Phi}_m}{2k_{Fe} l' \hat{B}_{y,s}} \tag{4}$$

$$h_{y,r} = \frac{\hat{\Phi}_m}{2k_{Fe} l' \hat{B}_{y,r}} \tag{5}$$

Due to the various SPPMSM winding forms, there are also various geometries for SPPMSM. In this paper, a wedge-shaped slot is assumed for the SPPMSM stator design. The angle of the wedge should be chosen appropriately. According to the SPPMSM design algorithm, both the number of the slot conductors (z_Q) and the stator current (I_s) are accessible, and hence, the height of the SPPMSM slot based upon (6) easily can be obtained by the two current density (J_s) and the number of slots (Q_s) parameters.

$$h_d = \frac{\left\{\frac{I_s z_Q}{J_s b_{u1}} + \frac{b_d}{2}\right\} Q_s}{\pi} \tag{6}$$

To calculate the inductance and the other SPPMSM parameters, it is required to specify the equivalent magnetic air gap. The length of the equivalent magnetic air gap is somewhat larger in absolute value than the geometric (or physical), and in the electrical machines, since it is one of the important parameters of magnetic energy exchange, it is very important to determine. Accordingly, this parameter should be calculated correctly.

Hence by a Carter coefficient (k_c):

$$k_c = \frac{\tau_u}{\tau_u - \kappa s} \tag{7}$$

With *s* same as the width of the slot opening, and κ:

$$\kappa = \frac{2}{\pi}\left\{\tan^{-1}\left(\frac{s}{2\delta}\right) - \frac{2\delta}{s}\log\sqrt{1-\left(\frac{s}{2\delta}\right)^2}\right\} \tag{8}$$

The effective SPPMSM magnetic air gap is produced by:

$$\delta' = k_c \times \delta \tag{9}$$

Following, the geometric dimensions of the SPPMSM slots which are taken into account in Fig 1 are calculated. On account of Fig. 1, the equivalent height (h_{eq}) of the stator slot of the SPPMSM and the width (w_{eq}) ones, correspondingly by (10) and (11) are given the following.

$$h_{eq} = \frac{y_4 + 2(y_1 + y_2 + y_3)}{2} \tag{10}$$

$$w_{eq} = \frac{x_1 + x_2}{2} \tag{11}$$

3- Initial Design

High energy density PMs and the development of power electronics instruments were the birth era of the PM machine in the late 1980s. After presenting the electromagnetic field excitation system by PMs and replacing it with conventional ones implements the following advantages [36]such as neodymium-iron-boron (NdFeB:

No excitation loss exists and so, higher efficiency is produced by not extracting electrical energy that makes losses.

- High power density
- High magnetic flux density produce in air-gap
- Proper dynamic performance
- High torque-to-size ratio
- Simplification of structure and maintenance by brushless.
- Reduced size and overall costs.
- Full-speed range, etc. [35].

As mentioned in the aforesaid sections, this paper aims to optimally design the SPPMSM to reduce torque ripple and the cogging torque as well as increase SPPMSM performance by improving its other parameters. In this section, a 1.5 kW, 4-pole, 36-slot SPPMSM with the parameters presented in Table 5 is designed in the first step (Fig. 2), and secondly

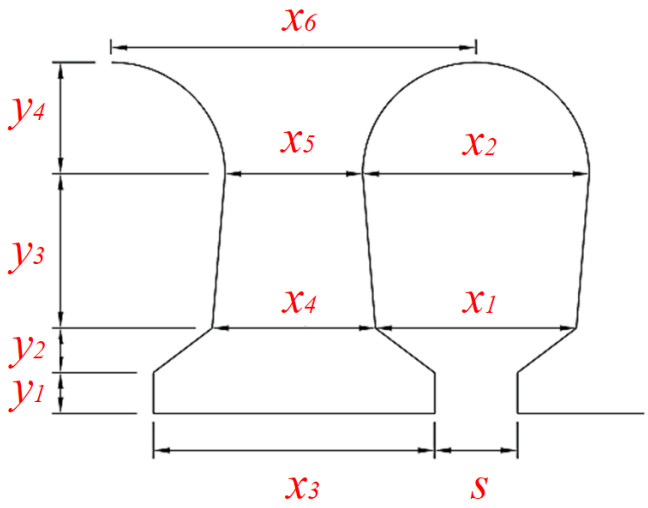

Fig. 1. Stator dimension of SPPMSM

Table 5. SPPMSM parameters and materials

Stator Outer Diameter	155 *mm*	PM Width	39 *mm*
Rotor Outer Diameter	104.4 *mm*	Stator Slots	36 (-)
Rotor Inner Diameter	38 *mm*	Pole Pairs	2 (-)
Air gap Length	0.8 *mm*	Rated Power	1.5 *kW*
PM Thickness	6 *mm*	Rated Current	2.5 *A*
Pole shoe width	152 *mm*	Stack Lenght	100 *mm*
Maximum Current	3.5 *A*	Rated Speed	1500 min^{-1}
Rotor and stator		S10C	
Winding		Copper	
PMs		NdFeB 38UH	

is optimized with the proposed three-step skewed pole shoe method. With respect to Table 5, in Fig. 2, the results of FEM of the designed SPPMSM are illustrated. As shown in Fig. 2, the designed SPPMSM has a rotor made of S10C steel which has been reported for use in SPPMSMs in many papers. The stator also includes the back-iron and 36 slots providing the three-phase winding. The SPPMSM electromagnetic model is designed and implemented with the following assumptions:

The flux density has only a radial direction.

MMF drop in the assumptive path above the stator and rotor irons of the SPPMSM was neglected.

Magnetic saturation does not occur during the machine electromagnetic analysis.

The no-load analysis of the machine is as Fig. 2, in the initially designed term.

4- Proposed Method

Respect to the specific rotor pole-shoe shape of the SPPMSMs as well as the technology required to manufacture the stator and the rotor sheets make the design and manufacturing of such machines challenging. This machines has many advantages such as high efficiency, high power density, better dynamic performance, etc, so-that are widely used in various types of industrial applications. So, the how-to performance of the SPPMSM is very important. In this section, a three-step skewed pole shoe method to re-design and optimize the before-section presented machine is accessible. The before-mentioned three-step skewed pole shoe method is compared with the initial method (non-optimized method) and the results are reported. Reaching this goal, Fig. 3 illustrates the three-step skewed pole shoe method, and next, the results of FEM for;

- Cogging torque
- Airgap flux density
- Back-EMF
- Average torque

are presented. Concerning Fig. 3, and designed SPPMSM with parameters tabulated in Table 5, the results of the optimally designed machine are presented following.

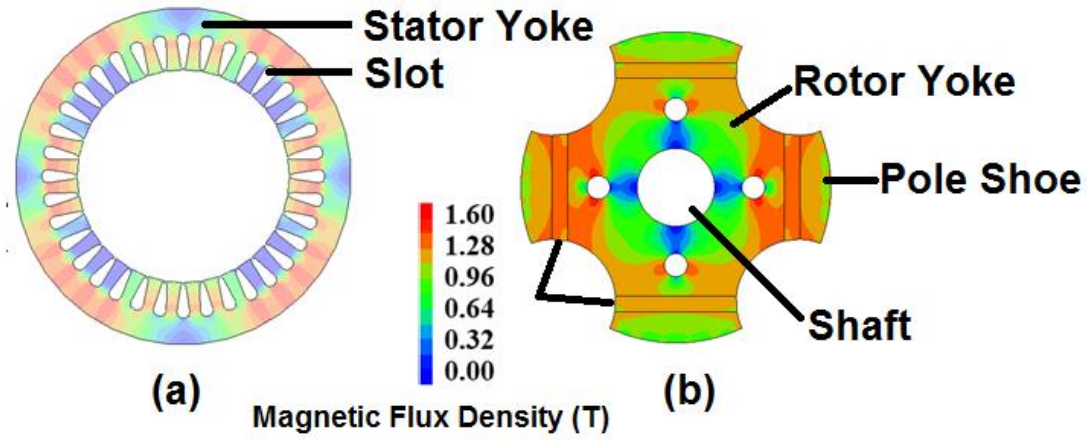

Fig. 2. No-load FEM results. a: stator, b: rotor

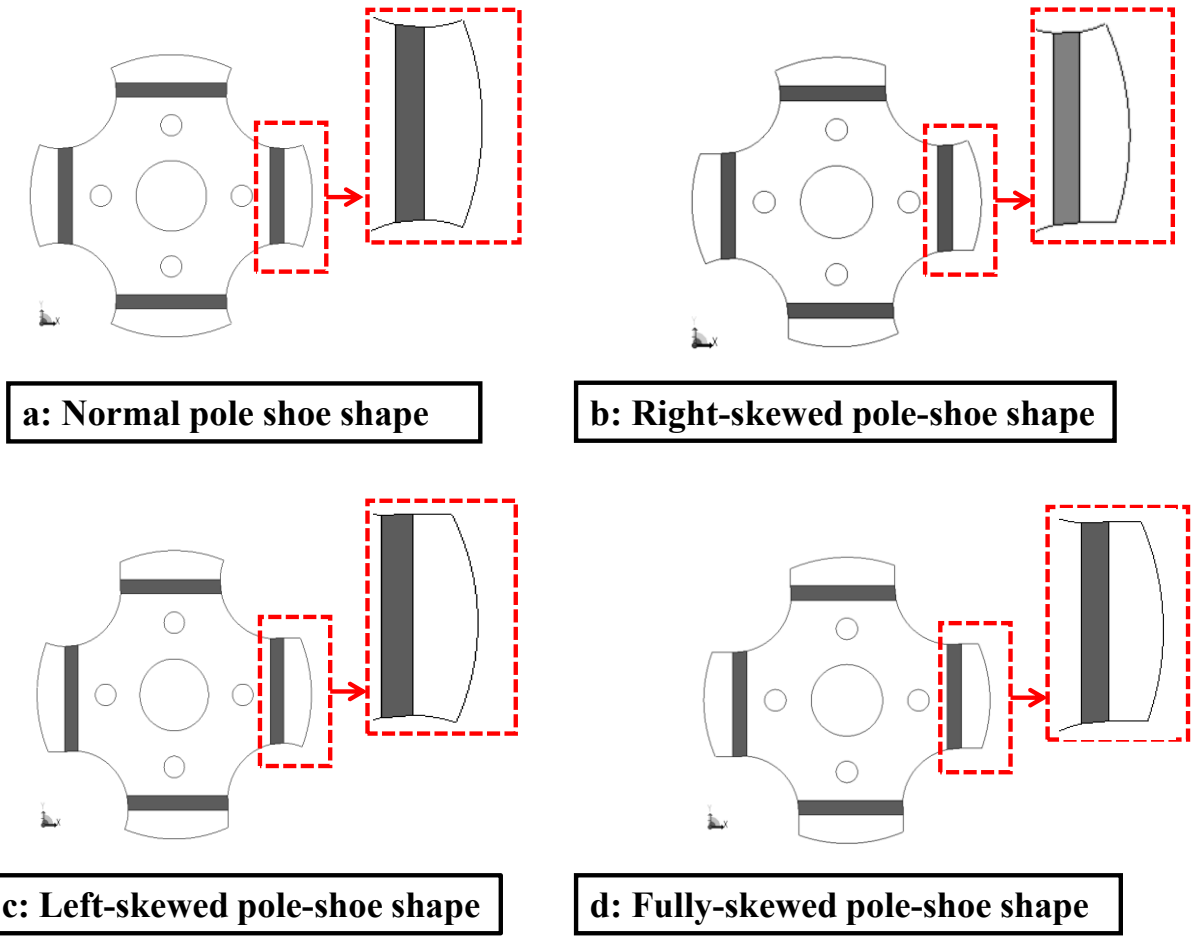

Fig. 3. The conventional method (a) and the three-skewed pole shoe shape (b, c and d)

5- Comparison of the Initial and Proposed Method

The design process of the SPPMSM, rotor, and stator shape, the proposed skewed pole shoe shape, and the performance of the designed machine are explored in this section. Accurate electromagnetic modeling of the SPPMSMs requires the use of FEM analysis that can be used to simulate even complex machine structures and obtain highly accurate results. Simulation of SPPMSM requires comprehensive and complete details of its structure. In a simulation, an accurate model with acceptable computational efficiency is required models. Clearly, these models often do not provide acceptable and appropriate information about the behavior of the SPPMSMs (for example torque ripple, cogging torque, etc.). Hence, the FEM is utilized for this goal. The FEM provides relatively ac

geometric structure, etc. In this way, JMAG has answered the requirements. The simulation process is time-consuming, mainly when re-design and the optimization of the SPPMSMs are considered, and as a result, the simulations have to be implemented for different geometric shapes of the SPPMSM based on the three-step skewed pole shoe method that is shown in Fig. 3. In the design, simulation, and optimization of electric machines, analytical methods can be coupled with FEM analysis, therefore the simulation and optimization timing reduces significantly. The 1.5 kW, 4-pole, 36-slots SPPMSM has a conventional stator pole shoe shape (normal pole shoe shape). Following, the results of the three-step skewed pole shoe method applied to the SPPMSM approaches are summarized and the design process of the proposed approach is as shown in a flow-chart as Fig. 4. With respect to Fig. 4, in the first step, a 1.5 kW, 4-pole, 36-slots SPPMSM is designed by defining the initial design parameters presented in Section II (The PMs and the pole-shoe shapes, T_{avg}, n_m, V_L, I_L, and D_m) as an initial model. The FEM analysis is performed and after completing the optimization cycle, a proper and optimized model with dimensions reported in the next sections is specified and re-designed to have a more satisfactory performance than the initial design of the SPPMSM. As a first parameter, the change in the cogging torque of the SPPMSM in the three-step skewed pole shoe method is investigated. The cogging torque in PM machines is caused by a disturbance between the output flux of a PM and a change in the magnetic resistance angles of the stator. One of the disadvantages that appear in SPPMSMs after this phenomenon is noise and vibrations. In SPPMSMs, there is a natural magnetic attraction due to the existing of the PMs and the steels of the rotor and stator between the pole of PMs and back-iron. This attraction is different on account of the presence of different slots in the stator of the SPPMSM, and clearly, in parts of the SPPMSMs where the volume of steel is higher, the quantity of this magnetic attraction is greater. Hence, this parameter is so important in the design stage of the SPPMSM to reduce annoying parameters such as the noise and vibration in the SPPMSM, and also pulsating torque. Owing to the production of this annoying factor, the shape of the rotor of the SPPMSM plays an important and accentuated role in achieving the desired output torque. Firstly for simplification, with a sight at Fig. 3, the three-skewed pole shoe shapes of the SPPMSM are named **Right-skewed pole shoe shape: State I**, **Left-skewed pole shoe shape: State II** and, **Fully-skewed pole shoe shape: State III.** Accordingly, Fig. 5, compares the cogging torque in three-skewed pole shoe shapes of the SPPMSM. Based on this figure, the cogging torque in State I is $0.090^{Nm,}$ and with a 3.33% reduction in State II is equal to 0.087^{Nm} and finally with a 0.061^{Nm} unit and a 67.77% reduction, in State III is equal to 0.029^{Nm}. As well, the air gap flux density is the second parameter that is investigated as one of the important parameters for achieving the optimum design. Since the aforementioned parameter is an important factor in determining the EMF voltage of the machine, as well as output torque, achieving its optimum value is critical. Fig. 6, illustrates the change in the air gap flux density of the SPPMSM in the optimization process. Regarding Fig. 6, it can be seen that the value of air gap flux density in these proposed methods is approximately in the same range. It is located and has not made any visible changes. According to Fig. 6. the maximum value that is considered for State III, is equal to 0.478^{T} with an approximate reduction of 6.27% and 5.23% compared to State III, which occurs in State II and State I that are equal to 0.448^{T} and 0.453^{T}, respectively. The torque ripple of SPPMSMs, considering no mechanical problems in the installation of a PMs, as well as magnetic asymmetry, in addition to cogging torque, is also due to the spatial harmonics of the Back-EMF voltage component. Fig. 7, also considers the changes in the back-EMF of the proposed scheme in the no-load condition of the SPPMSM, with respect to Fig. 3. In state I, the back-EMF is equal to 154.96^{V} and in State II and State III, an increase occurs and this parameter is equal to 155.16^{V} and 155.30^{V} in both before-said states, respectively. As mentioned before, the main sources of electromagnetic noise and vibration in SPPMSMs are highly dependent on many parameters such as torque ripple, such as the structure of the stator slots, and the rotor pole shoes. Consequently, this parameter should be optimized by considering many goals. In this way, the last and most important parameter is presented in Fig. 8 (average torque) and Fig. 9 (torque ripple). The average torque of re-designed and optimized SPPMSM in State I is equal to 9.781^{T}. A 0.3% increase, in State II, is equal to 9.811^{T}, and finally, with 4.01% and 3.69% increases respectively in comparison to State I and State II, in State III, it is equal to 10.174^{T} at the higher level. During the next significant parameter to optimization of the type of the SPPMSM, the torque ripple change with reference to Fig. 9. The torque ripple in the State I, State II, and State III are equal to 13.49%, 15.53%, and 10.42% respectively.

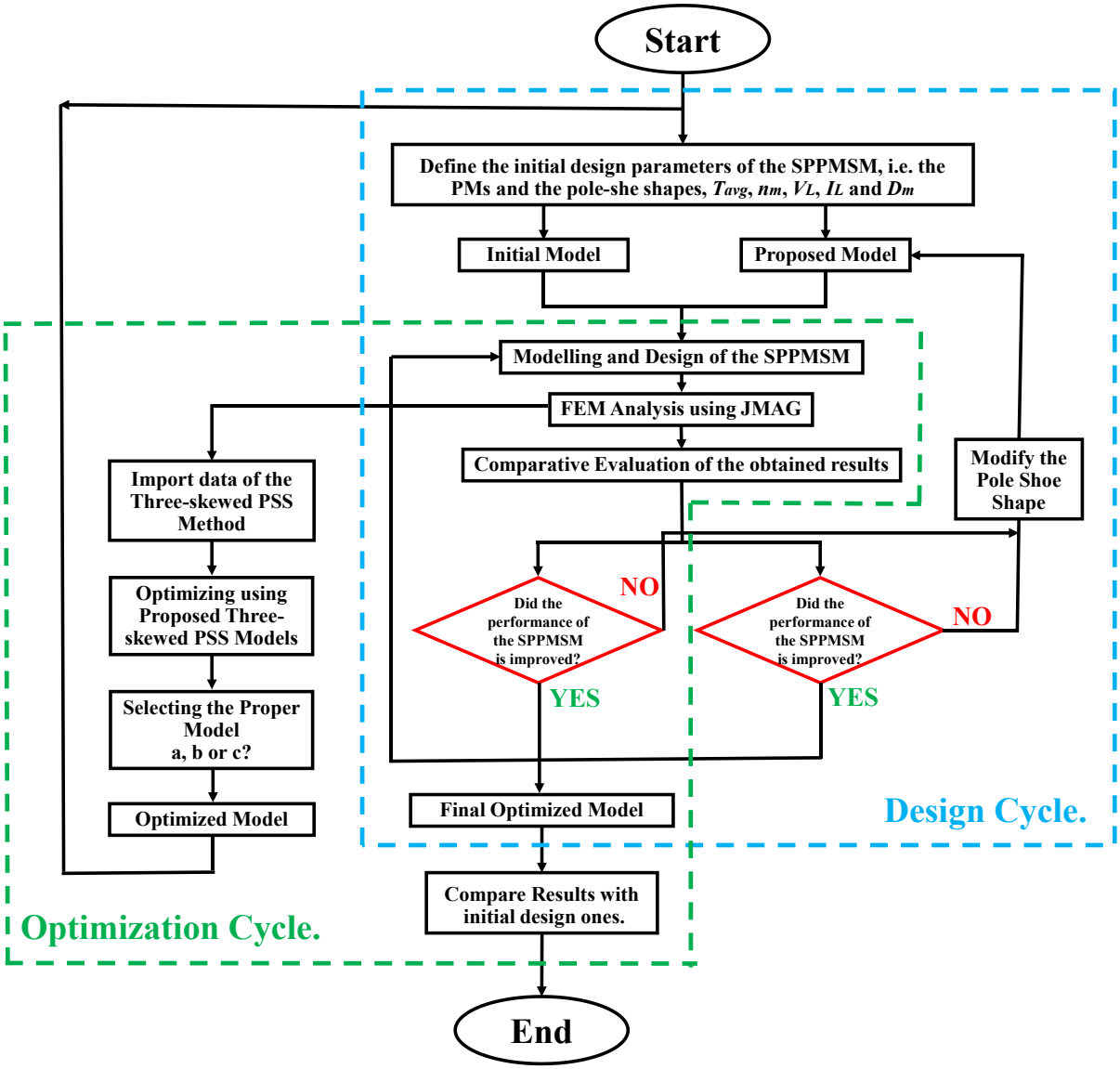

Fig. 4. Proposed Flow-chart

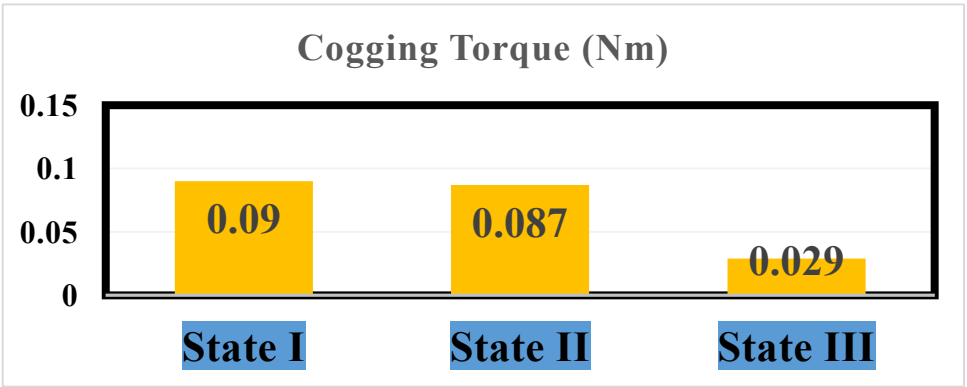

Fig . 5. The changing of the cogging torque in the proposed three-skewed pole shoe shapes

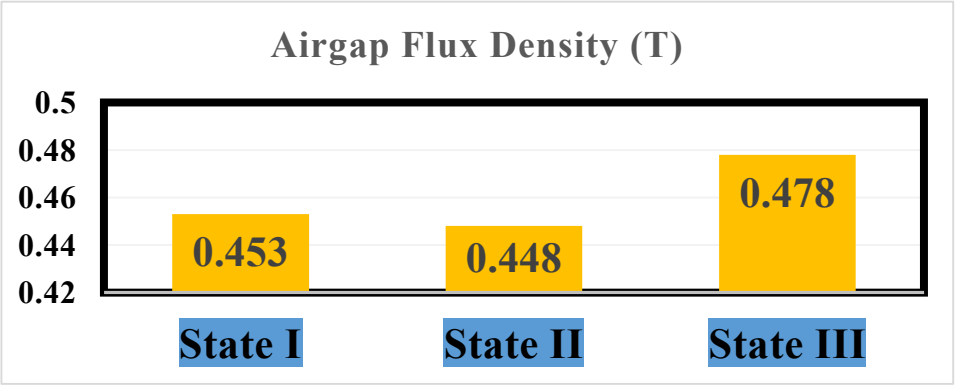

Fig . 6. The changing of the air gap flux density in the proposed three-skewed pole shoe shapes

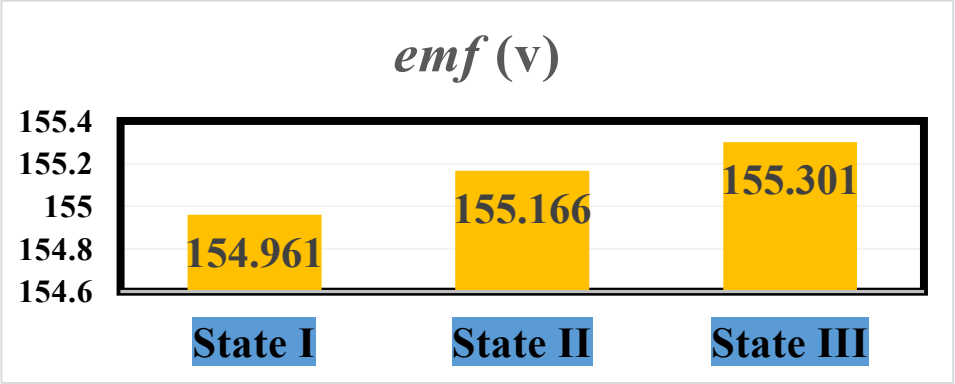

Fig . 7. The changing of the Back-EMF in the proposed three-skewed pole shoe shapes

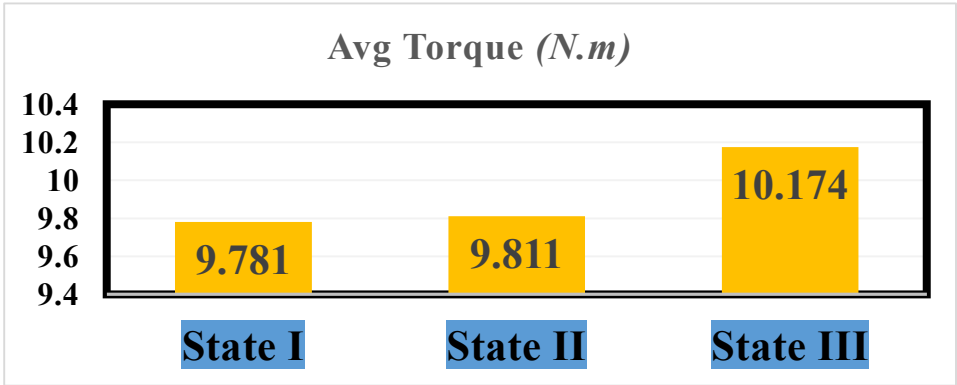

Fig . 8. The changing of the average torque in the proposed three-skewed pole shoe shapes

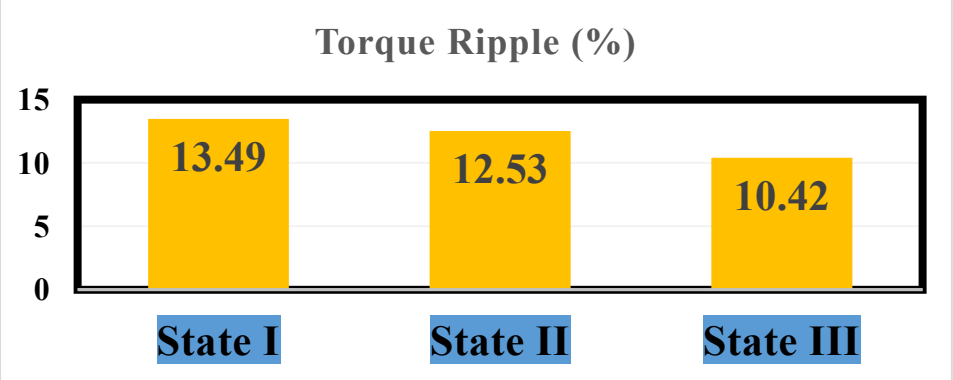

Fig . 9. The changing of the torque ripple in the proposed three-skewed pole shoe shapes

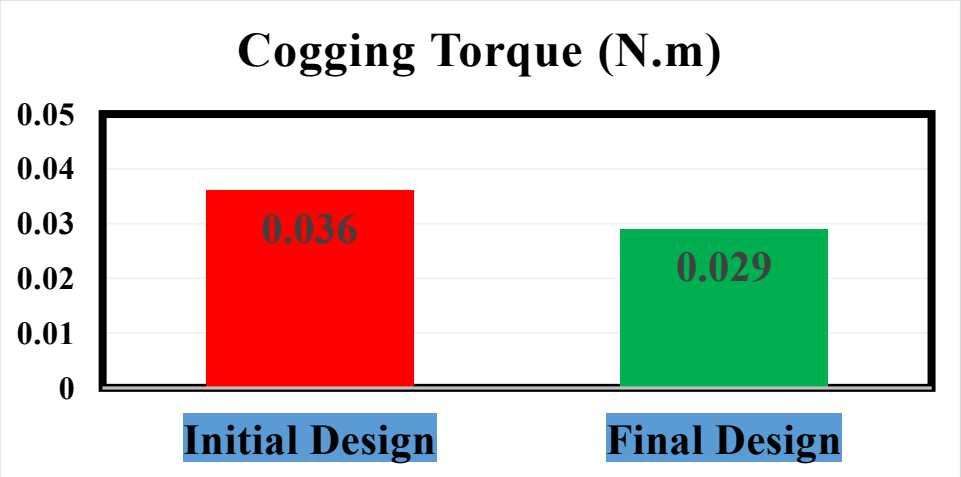

Fig . 10. Comparison between the cogging torque in the initial and the proposed design of the SPPMSM.

6- Results

In this section, the results of the three-skewed pole shoe shapes for optimizing the initial design of SPPMSM were reported. The goal is to select the proper one that ensures the electromagnetic operation of the machine in any operation condition with respect to improvement in other parameters of the SPPMSM, compared to the initial design scheme that presents an optimum scheme. The results reveal that in the three-skewed pole shoe shapes, the more proper scheme of the proposed methods is the State III, i.e. The Fully-Skewed pole-shoe shape. The FEM results of the re-designed the SPPMSM shows that in this scheme, the electromagnetic performance of SPPMSM is more proper than the previous two proposed schemes. So, in the following, the SPPMSM is re-designed based on the new pole-shoe shape, and the results of the proposed method are compared with the initial design of the SPPMSM, and it is reported next. For comparison, the cogging torque is the first choice. Owing to Fig. 10, the cogging torque in the initial design of the SPPMSM was 0.036^{T} and with a 19.44% reduction compared to the initial design, in the proposed final design is equal to 0.029^{T}. The second parameter is the back-EMF voltage in the proposed final design, it is equal to 155.301^{V} with a 1.27% increase in value with respect to Fig. 11. Another important parameter to re-design and optimization of the proposed SPPMSM is Torque. Torque plays an important role in the operation of the machine. Hence, this parameter should be accurately selected in the optimum value. Concerning Fig. 12, and Fig. 13, the average torque of the machine in the initial design and the proposed final scheme are equal to $9.911^{N.m}$ and $10.174^{N.m}$, respectively. It means a 2.65% increase in the total average torque. In the aspect of the torque ripple, a 16.03% reduction occurs. The torque ripple in the initial design of the SPPMSM, and final ones, are equal to 12.41% and 10.42%, respectively. Next, the FEM results of the proposed final design of the SPPMSM are presented. Accordingly, Fig. 14, and Fig. 15, show the cogging torque and the *phase-a* back-EMF voltage in the no-load operation of the initial and the finally designed machine, respectively. The output torque of the SPPMSM is also illustrated in Fig. 16 and compared to the initial design. A significant increase in output torque and also, a reduction in the ripple equal to 16.03% is accomplished due to the optimization process.

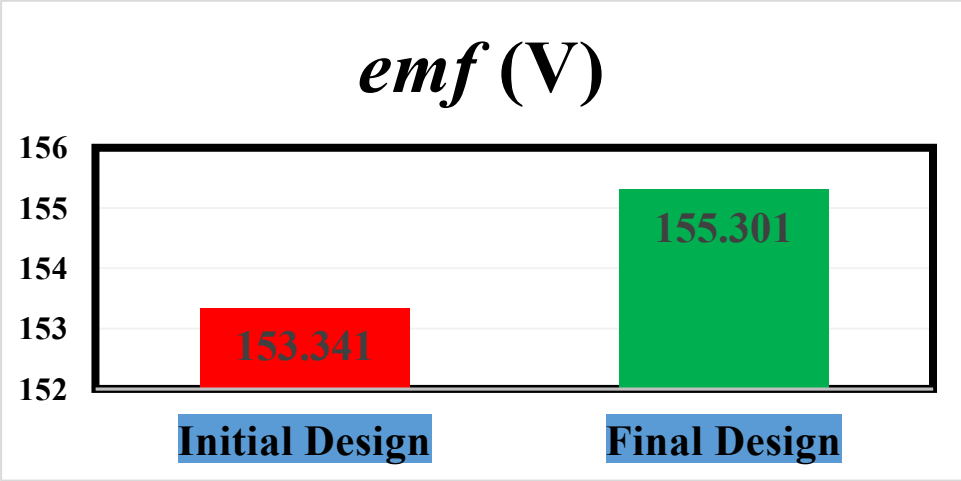

Fig . 11. Comparison between the Back-EMF in the initial and the proposed design of the SPPMSM.

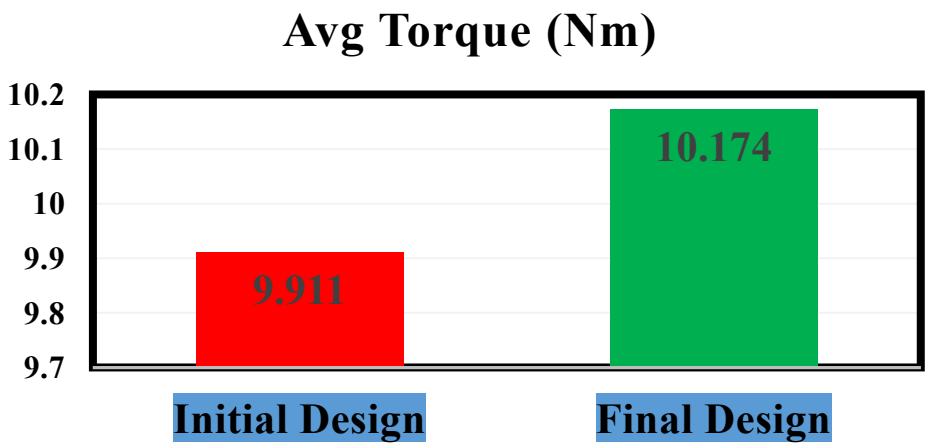

Fig . 12. Comparison between the average torque in the initial and the proposed design of the SPPMSM.

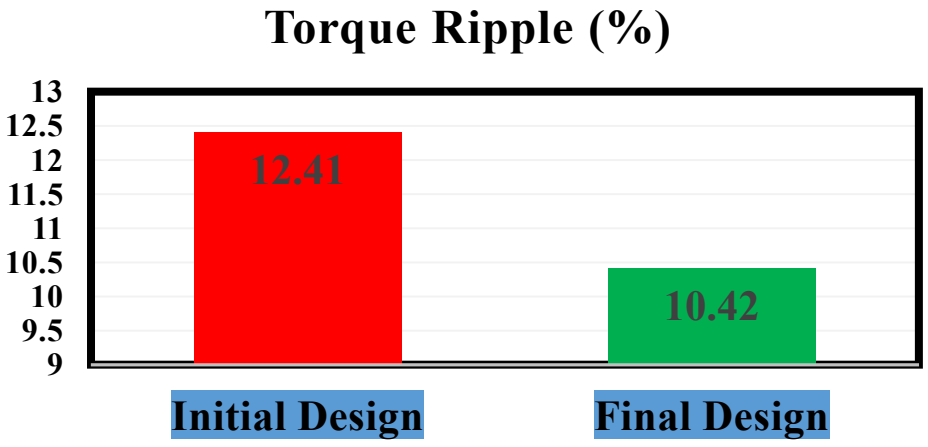

Fig . 13. Comparison between the torque ripple in the initial and the proposed design of the SPPMSM.

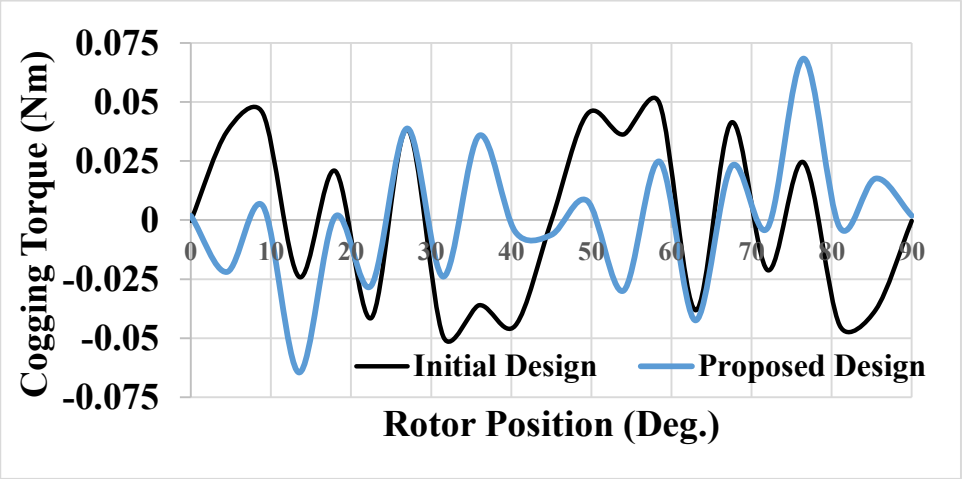

Fig . 14. Cogging torque in the initial design and the proposed design of SPPMSM

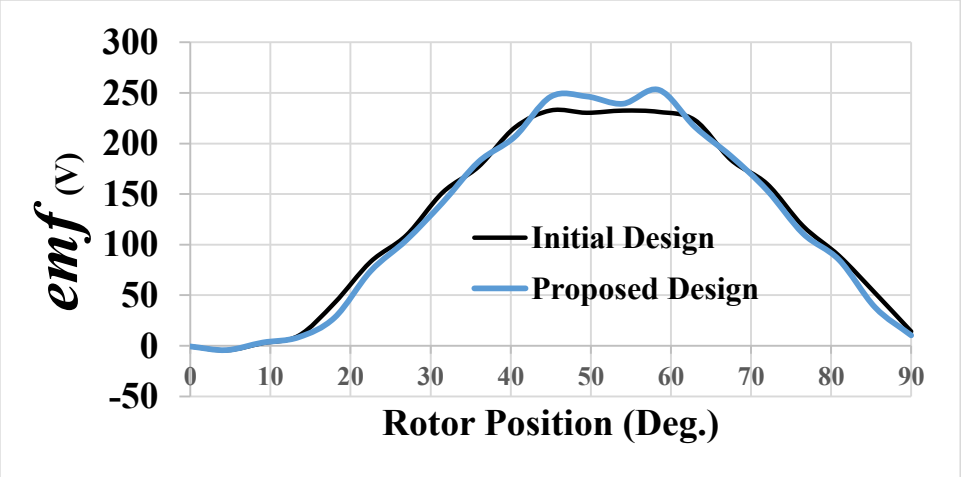

Fig . 15. Back-EMF in the initial design and the proposed design of SPPMSM

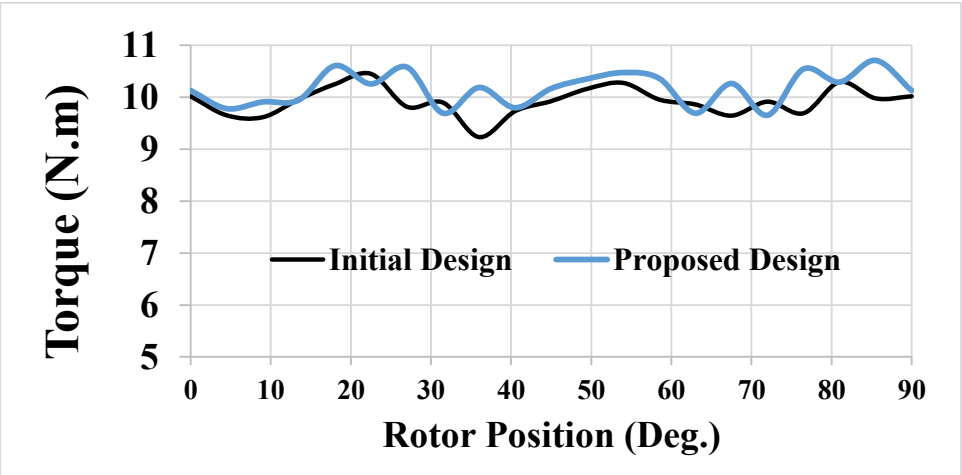

Fig . 16. Torque in the initial design and the proposed design of SPPMSM

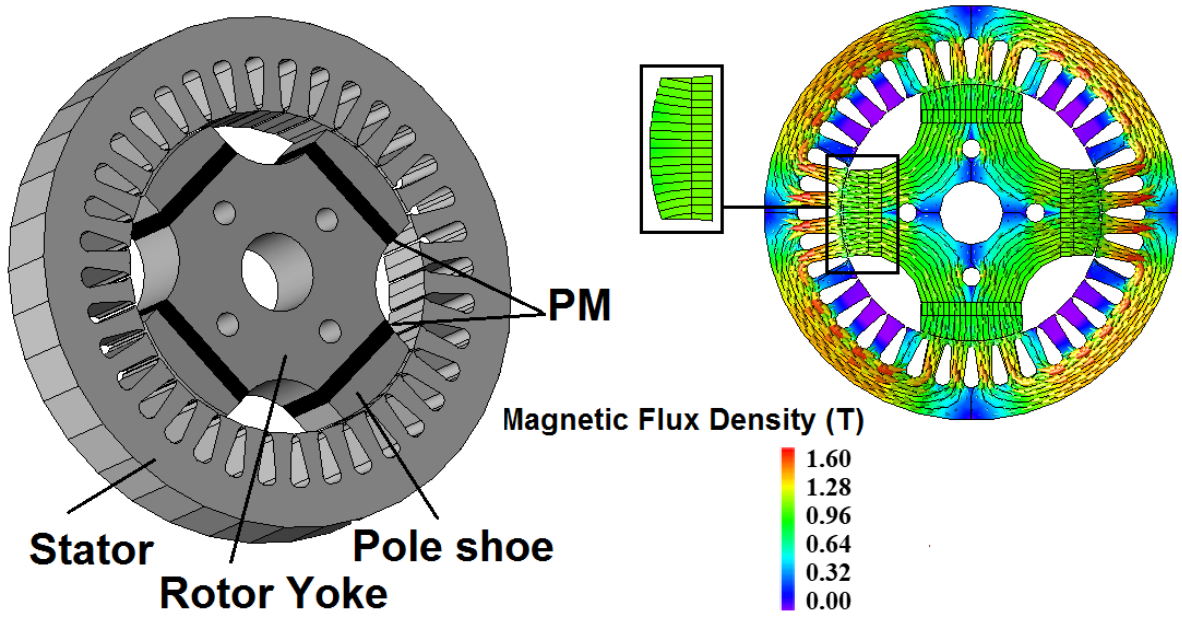

Fig . 17. The FEM results of the final designed SPPMMS

Finally, the 3D structure of the designed SPPMSM and the FEM result such as the no-load magnetic flux density and flux lines, have been shown in Fig. 17. Additionally, a significant torque ripple reduction is marked in the optimized model compared with the initial design. The average output torque is enhanced by 2.65% in the optimized model. In this way, the maximum torque is increased by 2.48% in the optimized model as compared to the initial one as displayed in Fig. 15. The minimum torque in the optimized model of the SPPMSM is also increased by 4.66% which leads to a low torque ripple compared to the initial design. A quantitative investigation of the parameters obtained from the initial and the optimized mode; of the SPPMSM shows the decreased torque ripples, cogging torque, and better-quality output torque of the aforementioned machine compared to the initial design one, and also, other parameters such as back-EMF voltage, airgap flux density, etc. have a better performance compared to the initial design of the machine. The optimized model showed better performance and operation characteristics compared to the initial model of the machine.

7- Conclusion

In the conventional structure of synchronous machines, the rotor has windings, in rare designs, it consists of PMs that are called SPPMSMs, which are investigated in this paper. The most important problem is methods to reduce ripple and improve torque in SPPMSMs. SPPMSMs have a special shape of the pole-shoe the design, assembly, and construction of these machines should be done with suitable consideration. Among the important factors of torque improvement, are the arrangement of the PMs in the rotor and the product of a reasonable deviation and deformation in the salient pole shoes. This issue is not considered in previous papers for this type of machine. There are many methods to design SPPMSMs with various advantages and disadvantages, but all of them focus on designing an SPPMSM while maintaining a balance between electromagnetic designs coupled with proper operating conditions. Owing to the many advantages of SPPMSMs such as high efficiency and power factor, high power density, and low vibration and noise, these machines are applicable in industrial, commercial, and also home applications. However relying on the technology required to manufacture the stator and the rotor sheet of these machines, as well as the specific rotor pole-shoe shape, make the research limited in the literature. Similarly, very few investigations led to the construction of prototypes of these machines. Most of the research performed was limited to academic activities. In this paper, at the first step, a 1.5 kW 4-pole, 36-slot SPPMSM is designed as the initial design. Next, a three-step skewed pole shoe method named: Right-skewed pole-shoe shape, Left-skewed pole-shoe shape, and Fully-skewed pole-shoe shape for re-design and optimizing of the SPPMSM to improve all-aspect parameters such as output torque, cogging torque, torque ripple, back-EMF, air gap flux density, etc. coupled with the improvement the electromagnetic and operation condition of the SPPMSM is presented. The FEM results show in the three-level proposed model, the Fully-skewed pole-shoe shape is proper and leads to improving the performance of the initial SPPMSM design. The significant results obtained are as follows:

- Average output torque is increased by 12.65%,
- The torque ripple is decreased by approximately 16.03%,
- The air gap flux density is increased by about 3.33%.
- The Back-EMF voltage in the initial design of the machine is equal to 155.341 V, and the optimized model is

equal to 155.301 i.e. a 1.27% increase,

- And finally, the cogging torque of the machine is reduced by 19.44%, compared to the initial design.

The related FEM results validated the electromagnetic performance of the finally designed machine at any predicted operation conditions. The proposed method presented in this paper can aid researchers and electrical machine designers associated with the SPPMSMs design and manufacture.

References

[1] B. Fonseca, J. O. P. Pinto, W. I. Suemitsu, R. C. Garcia, and M. L. M. Kimpara, "Torque Ripple Reduction Using Hierarchical-like Fuzzy Controller of a Five-Phase Salient Pole Permanent Magnet Synchronous Motor Drive," Conf. Rec. - IAS Annu. Meet. (IEEE Ind. Appl. Soc., vol. 2021-Octob, 2021, doi: 10.1109/IAS48185.2021.9677108.

[2] H. Parivar and A. Darabi, "Design and Modeling of a High-Speed Permanent Magnet Synchronous Generator with a Retention Sleeve of Rotor," Int. J. Eng., vol. 34, no. 11, pp. 2433–2441, Nov. 2021, doi: 10.5829/IJE.2021.34.11B.07.

[3] G. Dajaku and D. Gerling, "Air-Gap Flux Density Characteristics of Salient Pole Synchronous Permanent-Magnet Machines," IEEE Trans. Magn., vol. 48, no. 7, pp. 2196–2204, 2012, doi: 10.1109/TMAG.2012.2190144.

[4] Z. Shi et al., "Torque Analysis and Dynamic Performance Improvement of a PMSM for EVs by Skew Angle Optimization," IEEE Trans. Appl. Supercond., vol. 29, no. 2, Mar. 2019, doi: 10.1109/TASC.2018.2882419.

[5] H. Parivar and A. Darabi, "A Proposed Method to Rotordynamic Analysis of a High-speed Permanent Magnet Synchronous Machine by Retention Sleeve," SJEE, vol. 20, no. 2, pp. 269–281, Jun. 2023, doi: 10.2298/SJEE2302269P.

[6] H. Huang, D. Li, X. Ren, and R. Qu, "Analysis and Reduction Methods of Cogging Torque in Dual PM Vernier Machines with Unevenly Distributed Split Teeth," IEEE Trans. Ind. Appl., vol. 58, no. 4, pp. 4637–4647, 2022, doi: 10.1109/TIA.2022.3173896.

[7] J. Qi et al., "Suppression of Torque Ripple for Consequent Pole PM Machine by Asymmetric Pole Shaping Method," IEEE Trans. Ind. Appl., vol. 58, no. 3, pp. 3545–3557, 2022, doi: 10.1109/TIA.2022.3159629.

[8] M. Liu, X. Zhu, Z. Xiang, L. Quan, T. Wang, and T. Zhu, "Cogging Torque Reduction of Halbach Array Permanent Magnet Motor Based on Magnetic Field Energy Equivalence," Proc. 2021 IEEE 4th Int. Electr. Energy Conf. CIEEC 2021, May 2021, doi: 10.1109/CIEEC50170.2021.9510795.

[9] L. Wu, G. Ming, L. Zhang, and Y. Fang, "Improved Stator/Rotor-Pole Number Combinations for Torque Ripple Reduction in Doubly Salient PM Machines," IEEE Trans. Ind. Electron., vol. 68, no. 11, pp. 10601–10611, Nov. 2021, doi: 10.1109/TIE.2020.3032926.

[10] H. S. Zhang, M. L. Yang, Y. Zhang, J. Y. Tuo, S. Luo, and J. Xu, "Analytical Calculation of Surface-Inset PM In-Wheel Motors and Reduction of Torque Ripple," IEEE Trans. Magn., vol. 57, no. 1, Jan. 2021, doi: 10.1109/TMAG.2020.3034882.

[11] M. Yousuf, F. Khan, J. Ikram, R. Badar, S. S. H. Bukhari, and J. S. Ro, "Reduction of Torque Ripples in Multi-Stack Slotless Axial Flux Machine by Using Right Angled Trapezoidal Permanent Magnet," IEEE Access, vol. 9, pp. 22760–22773, 2021, doi: 10.1109/ACCESS.2021.3056589.

[12] W. Chen, J. Ma, G. Wu, and Y. Fang, "Torque Ripple Reduction of a Salient-Pole Permanent Magnet Synchronous Machine with an Advanced Step-Skewed Rotor Design," IEEE Access, vol. 8, pp. 118989–118999, 2020, doi: 10.1109/ACCESS.2020.3005762.

[13] H. Parivar and A. Darabi, "Taguchi Method for Design and Optimization of a High-Speed Permanent Magnet Synchronous Generator Protected by Retention Sleeve," http://www.sciencepublishinggroup.com, vol. 7, no. 2, p. 21, 2022, doi: 10.11648/J.EAS.20220702.12.

[14] W. Fei, P. C. K. Luk, and W. Liang, "Comparison of torque characteristics in permanent magnet synchronous machine with conventional and herringbone rotor step skewing techniques," ECCE 2016 - IEEE Energy Convers. Congr. Expo. Proc., 2016, doi: 10.1109/ECCE.2016.7854944.

[15] W. Fei and Z. Q. Zhu, "Comparison of cogging torque reduction in permanent magnet brushless machines by conventional and herringbone skewing techniques," IEEE Trans. Energy Convers., vol. 28, no. 3, pp. 664–674, 2013, doi: 10.1109/TEC.2013.2270871.

[16] O. Ocak and M. Aydin, "An Innovative Semi-FEA Based, Variable Magnet-Step-Skew to Minimize Cogging Torque and Torque Pulsations in Permanent Magnet Synchronous Motors," IEEE Access, vol. 8, pp. 210775–210783, 2020, doi: 10.1109/ACCESS.2020.3038340.

[17] X. Sun et al., "Skew angle optimization analysis of a permanent magnet synchronous motor for EVs," Proc. 2018 IEEE Int. Conf. Appl. Supercond. Electromagn. Devices, ASEMD 2018, Dec. 2018, doi: 10.1109/ASEMD.2018.8558826.

[18] M. Mirzaei Alavijeh and S. Shamlou, "A quantitative comparison among different types of auxiliary slot, auxiliary tooth, and the slot opening in split-pole Vernier machine," Electr. Eng., vol. 102, no. 3, pp. 1483–1492, Sep. 2020, doi: 10.1007/S00202-020-00969-W/FIGURES/12.

[19] H. Parivar, S. M. Seyyedbarzegar, and A. Darabi, "An Improvement on Slot Configuration Structure of a Low-Speed Surface-Mounted Permanent Magnet Synchronous Generator with a Wound Cable Winding," Int. J. Eng., vol. 34, no. 9, pp. 2045–2052, Sep. 2021, doi: 10.5829/IJE.2021.34.09C.01.

[20] A. Kioumarsi, M. Moallem, and B. Fahimi, "Mitigation of torque ripple in interior permanent magnet motors by optimal shape design," IEEE Trans. Magn., vol. 42, no. 11, pp. 3706–3711, Nov. 2006, doi: 10.1109/TMAG.2006.881093.

[21] G. H. Lee, S. Il Kim, J. P. Hong, and J. H. Bahn, "Torque Ripple reduction of interior permanent magnet synchronous motor using harmonic injected current," IEEE Trans. Magn., vol. 44, no. 6, pp. 1582–1585, Jun.

2008, doi: 10.1109/TMAG.2008.915776.

[22] S. H. Han, T. M. Jahns, W. L. Soong, M. K. Güven, and M. S. Illindala, "Torque ripple reduction in interior permanent magnet synchronous machines using stators with odd number of slots per pole pair," IEEE Trans. Energy Convers., vol. 25, no. 1, pp. 118–127, Mar. 2010, doi: 10.1109/TEC.2009.2033196.

[23] J. Kwack, S. Min, and J. P. Hong, "Optimal stator design of interior permanent magnet motor to reduce torque ripple using the level set method," IEEE Trans. Magn., vol. 46, no. 6, pp. 2108–2111, 2010, doi: 10.1109/TMAG.2010.2044871.

[24] G. H. Kang, Y. D. Son, and G. T. Kim, "A novel cogging torque reduction method for interior type permanent magnet motor," Conf. Rec. - IAS Annu. Meet. (IEEE Ind. Appl. Soc., pp. 119–125, 2007, doi: 10.1109/IAS.2007.4347776.

[25] K. C. Kim, D. H. Koo, J. P. Hong, and J. Lee, "A study on the characteristics due to pole-arc to pole-pitch ratio and saliency to improve torque performance of IPMSM," IEEE Trans. Magn., vol. 43, no. 6, pp. 2516–2518, 2007, doi: 10.1109/TMAG.2007.893524.

[26] C. A. Borghi, D. Casadei, A. Cristofolini, M. Fabbri, and G. Serra, "Application of a multiobj active minimization technique for reducing the torque ripple in permanent-magnet motors," IEEE Trans. Magn., vol. 35, no. 5 PART 3, pp. 4238–4246, 1999, doi: 10.1109/20.799073.

[27] D. Lin, S. L. Ho, and W. N. Fu, "Analytical prediction of cogging torque in surface-mounted permanent-magnet motors," IEEE Trans. Magn., vol. 45, no. 9, pp. 3296–3302, Sep. 2009, doi: 10.1109/TMAG.2009.2022398.

[28] R. Islam, I. Husain, A. Fardoun, and K. McLaughlin, "Permanent-magnet synchronous motor magnet designs with skewing for torque ripple and cogging torque reduction," IEEE Trans. Ind. Appl., vol. 45, no. 1, pp. 152–160, 2009, doi: 10.1109/TIA.2008.2009653.

[29] D. Žarko, D. Ban, and T. A. Lipo, "Analytical solution for cogging torque in surface permanent-magnet motors using conformal mapping," IEEE Trans. Magn., vol. 44, no. 1, pp. 52–65, 2008, doi: 10.1109/TMAG.2007.908652.

[30] N. K. Endla, "Analytically determined graph based solution for minimum cogging in spm motors with integer slots per pole," 2019 IEEE Int. Electr. Mach. Drives Conf. IEMDC 2019, pp. 1325–1329, May 2019, doi: 10.1109/IEMDC.2019.8785237.

[31] T. Hong, X. Bao, W. Xu, J. Fang, and Y. Xu, "Reduction of Cogging Torque by Notching Groove on Magnets in SMPMSM," 2019 22nd Int. Conf. Electr. Mach. Syst. ICEMS 2019, Aug. 2019, doi: 10.1109/ICEMS.2019.8921986.

[32] X. Wang, Y. Yang, and D. Fu, "Study of cogging torque in surface-mounted permanent magnet motors with energy method," J. Magn. Magn. Mater., vol. 267, no. 1, pp. 80–85, Nov. 2003, doi: 10.1016/S0304-8853(03)00324-X.

[33] K. Y. Hwang, J. H. Jo, and B. I. Kwon, "A study on optimal pole design of spoke-type ipmsm with concentrated winding for reducing the torque ripple by experiment design method," IEEE Trans. Magn., vol. 45, no. 10, pp. 4712–4715, 2009, doi: 10.1109/TMAG.2009.2022645.

[34] W. Zhao, T. A. Lipo, and B. Il Kwon, "Torque Pulsation Minimization in Spoke-type Interior Permanent Magnet Motors with Skewing and Sinusoidal Permanent Magnet Configurations," IEEE Trans. Magn., vol. 51, no. 11, Nov. 2015, doi: 10.1109/TMAG.2015.2442977.

[35] E. Sulaiman, G. M. Romalan, and N. A. Halim, "Skewing and notching configurations for torque pulsation minimization in spoke-Type interior permanent magnet motors," ICCEREC 2016 - Int. Conf. Control. Electron. Renew. Energy, Commun. 2016, Conf. Proc., pp. 202–207, Jan. 2017, doi: 10.1109/ICCEREC.2016.7814984.

[36] B. Poudel, E. Amiri, P. Rastgoufard, and B. Mirafzal, "Toward Less Rare-Earth Permanent Magnet in Electric Machines: A Review," IEEE Trans. Magn., vol. 57, no. 9, Sep. 2021, doi: 10.1109/TMAG.2021.3095615.

HOW TO CITE THIS ARTICLE

H. Parivar, A. Darabi, Optimization and Torque Improvement of a Salient-Pole Permanent Magnet Synchronous Machine by Three-step Skewed Pole Shoe Method, AUT J. Elec. Eng., 56(1) (Special Issue) (2024) 125-140.

DOI: 10.22060/eej.2024.22513.5544